

Structured ZSM-5/SiC foam catalysts for bio-oils upgrading

Ou, X., Wu, C., Shi, K., (...), Jiao, Y., Fan, X.



**University of
Nottingham**
UK | CHINA | MALAYSIA

University of Nottingham Ningbo China, 199 Taikang East Road, Ningbo, 315100, China

First published 2020

This work is made available under the terms of the Creative Commons Attribution 4.0 International License:

<http://creativecommons.org/licenses/by/4.0>

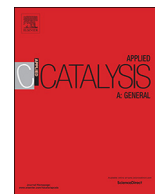
The work is licenced to the University of Nottingham Ningbo China under the Global University Publication Licence:

<https://www.nottingham.edu.cn/en/library/documents/research-support/global-university-publications-licence.pdf>



**University of
Nottingham**

UK | CHINA | MALAYSIA



Structured ZSM-5/SiC foam catalysts for bio-oils upgrading

Xiaoxia Ou^a, Chunfei Wu^b, Kaiqi Shi^c, Christopher Hardacre^a, Jinsong Zhang^d, Yilai Jiao^{d,*}, Xiaolei Fan^{a,*}

^a Department of Chemical Engineering and Analytical Science, School of Engineering, The University of Manchester, Oxford Road, Manchester, M13 9PL, United Kingdom

^b School of Chemistry and Chemical Engineering, Queen's University Belfast, Belfast, BT7 1NN, United Kingdom

^c New Materials Institute, The University of Nottingham Ningbo China, Ningbo, 315100, China

^d Shenyang National Laboratory for Materials Science, Institute of Metal Research, Chinese Academy of Sciences, 72 Wenhua Road, Shenyang, 110016, China

ARTICLE INFO

Keywords:

ZSM-5
SiC foam
Bio-oils upgrading
Coke formation
Deactivation mechanism
Process intensification

ABSTRACT

ZSM-5 zeolite coating supported on SiC foams was prepared by a precursor dispersion-secondary growth method and the resulting structured ZSM-5/SiC foam catalyst was used for the proof-of-concept study of catalytic bio-oils upgrading (*i.e.* deoxygenation of the model compounds of methanol and anisole) in reference to ZSM-5 catalyst pellets. A layer of ZSM-5 coating with inter-crystal porosity on SiC foams was produced by curing the zeolite precursor thermally at 80 °C. The use of SiC foam as the zeolite support significantly improved transport phenomena compared to the packed-bed using ZSM-5 pellets, explaining the comparatively good catalytic performance achieved by the structured ZSM-5/SiC foam catalyst. In comparison with the ZSM-5 pellets, the ZSM-5/SiC foam catalyst showed 100.0% methanol conversion (at the weight hourly space velocity, WHSV, of 8 h⁻¹) and 100.0% anisole conversion (at WHSV = 5 h⁻¹) at the initial stage of the processes, while only about 3% were obtained for the ZSM-5 pellets, under the same conditions. Based on the comparative analysis of the characterisation data on the fresh and spent catalysts, the deactivation mechanisms of the ZSM-5/SiC and the ZSM-5 pellet catalysts were explained. The process intensification using SiC foam to support ZSM-5 improved the global gas-to-solid mass transfer notably, and hence mitigating the pore blocking due to the carbon deposition on the external surface of supported ZSM-5.

1. Introduction

Bio-oils from the fast pyrolysis of biomass have the potential to be converted into fuels and chemicals, addressing the issues associated with the usage and shortage of fossil fuels [1], especially environmental ones such as airborne particulates, carbon dioxide (CO₂), sulphur oxides (SO_x) and nitrogen oxides (NO_x). Theoretically, bio-oils are CO₂ neutral, as well as containing much less bonded sulphur and nitrogen than fossil fuels. Thus, using bio-oils can significantly reduce the emissions of hazardous air pollutants [2]. However, bio-oils from biomass pyrolysis cannot be used directly due to their undesired properties, such as high water content, high viscosity, high ash content and low chemical stability [3]. Additionally, bio-oils are complex mixtures of oxygenated compounds with a high oxygen content of *ca.* 38 wt.%, leading to the corrosion issues and low efficiency as fossil fuel derived oil replacements. For example, bio-oils derived from pyrolysis of wood only have heating values of 16–19 MJ kg⁻¹, and are, therefore, ineffective energy carriers compared to the heavy petroleum fuel oils with a heating value about 40 MJ kg⁻¹ [4]. Therefore, without the removal

of a large amount of oxygen from bio-oils [2], it is difficult to realise their potential as alternatives for fossil fuel and feedstock [5,6]. Thus, there is considerable interest in developing technologies to upgrade the bio-oils such as catalytic hydrodeoxygenation, HDO [7,8], deoxygenation, decarboxylation, decarbonylation and cracking [2,9–15]. After removing oxygen, bio-oils can be used efficiently for heat and power generation, as value-added platform chemicals (*e.g.* olefins [16,17]) or as transportation fuels [18]. For example, acetic acid can be catalytically converted to acetate or acetyl species, then upgraded into methane (CH₄) *via* decarboxylation or decarbonylation [19], and ethylene can be produced directly from acrolein (doubly dehydrated glycerol) *via* decarbonylation reactions over fluid catalytic cracking (FCC) catalysts [15].

HDO technology uses precious metal catalysts such as ruthenium and palladium and a large amount of hydrogen at elevated pressures up to 20 MPa [7,8]. Instead, catalytic deoxygenation and cracking reactions of bio-oils employs economic zeolites (*e.g.* ZSM-5 and zeolite Y) as the solid acid catalysts [1,2,13,14,20] and is operated at atmospheric pressure without the requirement of hydrogen, making it attractive

* Corresponding authors.

E-mail addresses: ylijiao@imr.ac.cn (Y. Jiao), xiaolei.fan@manchester.ac.uk (X. Fan).

<https://doi.org/10.1016/j.apcata.2020.117626>

Received 29 September 2019; Received in revised form 3 May 2020; Accepted 9 May 2020

Available online 13 May 2020

0926-860X/ © 2020 The Authors. Published by Elsevier B.V. This is an open access article under the CC BY license

(<http://creativecommons.org/licenses/by/4.0/>).

concerning the costs and safety. In zeolites, the Brønsted acid sites promote the deoxygenation and cracking reactions *via* the carbonium ion mechanism to produce the highly deoxygenated compounds such as aromatic oils and hydrocarbons [2,13]. ZSM-5 zeolite is one of the common cracking catalysts for upgrading bio-oils, producing high yields of desired hydrocarbons because of its particular three-dimensional medium-sized channel topology [2,7,11,13,14,21]. However, in practice, ZSM-5 zeolite is usually used as pellets in the packed-bed configuration. The pelletisation of ZSM-5 reduces the effective reaction surface and accessibility to active sites due to flow maldistribution [22,23], resulting in severe catalyst deactivation during bio-oil upgrading (e.g. over 30 wt.% of the wood-derived bio-oil remained as cokes over HZSM-5 [24], and the coke deposition at 12.15 wt.% was measured after the deactivation of HZSM-5 in the upgrading of biomass-derived bio-oils in the vapour phase [25]). Also, due to the high-pressure drop across the packed bed, the mass transfer between zeolite particles (within the pellets) is also restricted. A typical example is methanol-to-propylene (MTP) process over ZSM-5 pellets, in which the diffusion of propylene (*i.e.* the main product) is hindered within the zeolite pellets packing, promoting consecutive reactions such as oligomerisation and cyclisation [26,27]. Besides, as MTP is highly exothermic, the undesirable 'hot spot' is formed easily due to the inefficient heat transfer and then rapidly deactivates the zeolite catalyst [22,26,28–30].

Coating the zeolite on appropriate matrices (*i.e.* one of the structured zeolite catalysts) can provide good access of reactants to active sites and improve the transport phenomena, and hence enhance the efficiency and stability of the catalyst [22,26,31]. Therefore, structured zeolite catalysts can be good candidates for intensifying the catalytic upgrading of bio-oils. Structured open-cell foams, especially silicon carbide (SiC) foams, are good catalyst supports for process intensification due to their intrinsic (e.g. high thermal conductivity of SiC [30]) and structural properties (e.g. high open porosity and irregular pore structure [32–34]). These intrinsic pore structures generally promote the global mass transfer across the foam beds [26,32,33]. Besides, by rationally engineering the layer of catalyst, the local mass transfer across the catalyst coating layer on foam can be improved as well.

Zeolite coatings have been supported on SiC foams using various preparation methods including dip-coating [28,30,31] and direct hydrothermal synthesis [26,35,36], which all have advantages and disadvantages. For example, dip-coating is relatively simple, but it requires inert binders which may reduce the accessibility to the active sites in the zeolite [28,30]. Hydrothermal synthesis promotes the formation of pure zeolitic phases with good adhesion [35,36], but the deposition phenomena under hydrostatic conditions are prone to produce non-uniform coatings, even pore blocking [26]. Although the seed-facilitated secondary growth method can promote the selective growth of zeolites on foam supports [34,37], the resulting dense coating with intergrown zeolite crystals may impose additional mass transfer resistance during application due to the low porosity and accessibility. Accordingly, the difference among resulting zeolitic coatings is manifest in the porosity of coating layer (e.g. inter-crystal and intracrystal pores), crystal orientation, adherence strength (between coating and support), the degree of coverage and coating thickness [38], as well as the acidic characteristics of the coating.

In continuous-flow catalysis, a highly accessible zeolitic phase in the coating is preferred to reduce the diffusion resistance [39–41]. We have recently proved that the presence of inter-crystal pores in the zeolite coating contributes to the improved accessibility to the active phase, and thus benefiting the mass transfer and catalysis [30]. Zeolite precursor (*i.e.* amorphous aluminosilicate) was used as the binder to dip-coat ZSM-5 zeolite on SiC foams and subsequently converted to a zeolitic phase using a vapour-phase transport method (using steams containing tetrapropylammonium hydroxide, TPAOH) to create inter-crystal porosity [30]. A precursor dispersion-secondary growth method has been developed for preparing zeolite coating on SiC foams

[26,31,42]. In the preparation process, the conversion of zeolite precursors into zeolite phases is *via* dissolution-recrystallisation in the secondary growth synthesis [43–45], as illustrated in Fig. S1. It is proposed that the property of the precursor and the treatment of the dispersed precursor play important roles in the dissolution-recrystallisation process, thus affecting the properties of the coated zeolite. For example, an amorphous silica gel precursor was more beneficial than a semi-crystallised precursor to form a homogeneous coating of zeolite because the dissolution step was facilitated by the amorphous silica gel [42]. The heat treatment of zeolite precursor (*i.e.* the curing of the precursor on SiC foams) is another factor which influences the dissolution step because further phase change of the precursor may occur during the curing process. However, there is no study about the effect of precursor heat treatment temperature on the zeolite coating.

In this paper, we present the study of the effect of precursor thermal treatment temperature on the morphology of zeolite coatings on the surface of SiC foams. The resulting ZSM-5/SiC foam catalyst and a reference catalyst (ZSM-5 pellets catalyst) were subsequently tested for catalytic upgrading bio-oils (using methanol and anisole as the model compounds [46–48]) to compare the catalytic performance. A combination of nitrogen (N₂) physisorption, ammonia temperature-programmed desorption (NH₃-TPD) and thermogravimetric analysis (TGA) was used to compare and contrast the ZSM-5/SiC foam catalyst and ZSM-5 catalyst pellets (as-prepared and used ones) regarding their pore texture and acidity properties to understand their deactivation behaviours.

2. Experimental

2.1. Materials and synthesis of ZSM-5/SiC foam catalysts

Methanol and anisole (analytical grade) were purchased from Sinopharm Chemical Reagent Co., Ltd and used as received. Cylindrical SiC foams [26,31] (*i.e.* the structured catalyst supports) were used in the study (diameter = 25 mm, length = 50 mm) with the open-cell porosity of 60% and an open-cell diameter of about 1.5 mm (Fig. S2). The structural properties of bare SiC foams used in this work are summarised in Table S1.

The zeolite precursor (*i.e.* the silica gel or silicalite-1 seeds) was prepared using the conventional hydrothermal synthesis with a reaction mixture of tetraethoxysilane (TEOS, Sinopharm Chemical Reagent Co., Ltd), tetrapropylammonium hydroxide (TPAOH, 50% aqueous solution, China Haohua Chemical Group Co., Ltd), and deionised water (molar composition of TEOS:TPAOH:H₂O = 1:0.32:29) at 130 °C for 3 and 8 h, respectively. The precursor gel was dispersed on SiC foams by dip-coating (5 min under sonication). Then the precursor gel modified SiC foams were blown by air for a few seconds to remove the residual gel within the cellular structure and subsequently thermally treated in air for 12 h at 30, 80 and 200 °C (in a convective oven), respectively.

The secondary growth solution was prepared with a molar composition of Si:Al(NO₃)₃:TPAOH:H₂O = 1:0.025:0.112:108. The mixture of TEOS, TPAOH and H₂O was aged at room temperature under stirring for 3 h and Al(NO₃)₃ was then added. After stirring for 24 h, the aged secondary growth solution was transferred into a stainless-steel autoclave with a PTFE liner and the precursor modified SiC foam was immersed in the solution to allow the crystallisation at 175 °C for 48 h. The resulting samples were washed in deionised water at 100 °C under sonication for 40 min. The samples were dried at 100 °C for 12 h and calcined in a muffle furnace (temperature programme room temperature to 600 °C at 1 °C min⁻¹ then held at 600 °C for 6 h, to remove the template. The weight of the supported zeolite on SiC foam was determined by weighing the mass difference of the structured catalyst before (the dry foams) and after the synthesis (the calcined ZSM-5/SiC foams), showing that about 9.5 wt.% of ZSM-5 coating was supported on SiC foams. Both the supported ZSM-5 (on SiC foams) and ZSM-5 pellet have a theoretical Si/Al ratio of 40. The Si/Al ratio of the ZSM-5

layer supported on SiC foam was analysed by SEM-EDX, showing the ratio at ~ 30 (Fig. S3).

2.2. Characterisation of materials

X-ray diffraction (XRD) patterns were recorded on an X-ray diffractometer (Rigaku, D/max-2500/PC) using $\text{CuK}\alpha_1$ ($k = 1.5406 \text{ \AA}$) radiation at 50 kV and 200 mA. Morphologies of samples were observed using the scanning electron microscopy (SEM; Zeiss, SUPRA 35, Germany). Nitrogen (N_2) adsorption-desorption analysis of catalysts was performed at $-196.15 \text{ }^\circ\text{C}$ using a Micromeritics 3Flex Surface Characterization Analyser. Before the measurement, the catalysts (150 mg) were degassed at $350 \text{ }^\circ\text{C}$ under vacuum overnight. The specific surface area of materials was calculated using the Brunauer–Emmett–Teller (BET) method. Ammonia temperature-programmed desorption (NH_3 -TPD) was performed using a Micromeritics AutoChem II 2920 chemisorption analyser to measure the strength and concentration of acidic sites in zeolites. Before the analysis, about 100 mg catalyst was pre-treated at $550 \text{ }^\circ\text{C}$ for 1 h and then cooled down to $50 \text{ }^\circ\text{C}$ under Helium (He). Then, a gas mixture of NH_3 in He (10%:90%) was introduced at $30 \text{ cm}^3 \text{ min}^{-1}$ to saturate the catalyst followed by the purge of pure He ($60 \text{ cm}^3 \text{ min}^{-1}$) at $100 \text{ }^\circ\text{C}$ for 2 h to remove the physically adsorbed NH_3 . Finally, the desorption of chemisorbed NH_3 was enabled by heating the catalyst from $100 \text{ }^\circ\text{C}$ to $600 \text{ }^\circ\text{C}$ with a heating rate of $10 \text{ }^\circ\text{C min}^{-1}$ under He flow ($30 \text{ cm}^3 \text{ min}^{-1}$) and the desorbed NH_3 was monitored by a gas chromatography (GC) equipped with a thermal conductivity detector (TCD). Thermogravimetric analyses (TGA) of the spent catalysts were carried out using a Discovery TGA 550 analyser (TA Instruments) under air (flow rate = 50 mL min^{-1}) from $100 \text{ }^\circ\text{C}$ to $700 \text{ }^\circ\text{C}$ (at a heating rate of $10 \text{ }^\circ\text{C min}^{-1}$). Differential scanning calorimetry (DSC) thermal analysis of the spent catalysts (around 100 mg) was performed using a TA DSC 2500 calorimeter under N_2 (flow rate = 50 mL min^{-1}) from $100 \text{ }^\circ\text{C}$ to $395 \text{ }^\circ\text{C}$ (at a heating rate of $10 \text{ }^\circ\text{C min}^{-1}$). The variation of the open-cell porosity of the SiC foam before and after the deposition of ZSM-5 coating was measured using the displacement method (*i.e.* the measurement of water volume replaced by foams at room temperature). The reduction of the open-cell porosity of the foam after the coating synthesis was estimated as *ca.* 4% (from 60% to 56%).

2.3. Catalytic upgrading of bio-oil model molecules

The catalytic performance was evaluated using a fixed bed reactor at $400 \text{ }^\circ\text{C}$ and atmospheric pressure. In each run, the catalyst, *i.e.* the structured ZSM-5 on SiC foam catalyst (about 19 g total weight with *ca.* 9.5 wt.% of ZSM-5 coating layer, approximately 1.8 g zeolite) or 1.8 g ZSM-5 pellets, was packed in the reactor for the catalytic reactions. A thermocouple was affixed inside the reactor at the same position of the catalyst bed. Before the reaction, the catalyst bed was held at $400 \text{ }^\circ\text{C}$ for 0.5 h under N_2 (240 mL min^{-1}). The reactant (methanol or anisole) was fed by a peristaltic pump at different flow rates ($0.15\text{--}0.45 \text{ mL min}^{-1}$, with a constant N_2 /reactant volumetric ratio at 800) and vaporised before entering the reactor. All pipelines were maintained by a heating tape at $180 \text{ }^\circ\text{C}$ to avoid condensation. The reactants/products from the reactor were analysed online using gas chromatography (GC, Agilent 7890A) equipped with a flame ionisation detector (FID) and an HP-PLOT/Q capillary column (fused silica ID = 0.32 mm and length = 30 m). Peaks were identified by comparing their retention times to the reference standards, and the determination of percentage compositions was based on peak area normalisation method [49]. The determination of substrate conversion and product selectivity was provided in the Supporting Information (SI). The weight hourly space velocity (WHSV, h^{-1}) is defined as the ratio between the reactant mass flow rate and the mass of the ZSM-5 catalyst. The determination of coke formation from each experimental run was measured by weighing the catalyst before and after the reaction. The mass balance of the catalytic anisole

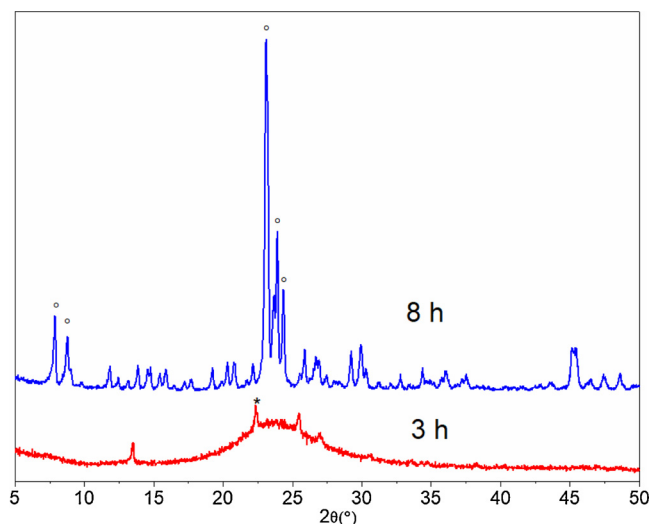


Fig. 1. XRD patterns of zeolite precursors by hydrothermal synthesis after 3 h (red line: predominantly amorphous silica gel along with some crystalline phases, *i.e.* silica with the amorphous diffraction peak at $22^\circ 2\theta$ [52]) and 8 h (blue line: crystallised silicalite-1 seeds with the characteristic MFI structure at about 7.9° , 8.8° , 23.1° , 24.0° and $24.5^\circ 2\theta$) (For interpretation of the references to colour in this figure legend, the reader is referred to the web version of this article).

upgrading process was estimated at about 90% (SI).

3. Results and discussion

3.1. ZSM-5/SiC foam catalyst with inter-crystal porosity

ZSM-5 precursors were synthesised at $130 \text{ }^\circ\text{C}$. Previous research showed that amorphous silica was the main phase of the precursor when the synthesis time was $< 5 \text{ h}$, while MFI seeds were formed with a synthesis time of $> 7 \text{ h}$ [42]. Therefore, 3 and 8 h were used in this work to prepare the ZSM-5 precursors for the surface modification of SiC foams. XRD (Fig. 1) and SEM results (Fig. 2a) show that the amorphous precursor gel was obtained after three-hour synthesis, whereas silicalite-1 seeds were formed by extending the synthesis time to eight hours (Figs. 1 and 2c), which is consistent with the results for the previous study [42]. For ZSM-5 coating originated from the crystallised seeds (Fig. 2c) dispersed on SiC foam, a dense layer of intergrown ZSM-5 crystals was observed, as shown in Fig. 2d. During the secondary growth synthesis, the well-crystallised seeds (Fig. 2c) grow directly into a layer of intergrown and interlocking crystals on the surface of SiC foam under the hydrothermal conditions [50,51]. When the precursor gel (Fig. 2a) was used to be dispersed on SiC foams, ZSM-5 coating with randomly orientated crystals ($2 \times 5 \times 15 \text{ }\mu\text{m}^3$) was formed accordingly after the secondary growth synthesis, in which inter-crystal voids were present, as shown in Fig. 2b. The dense zeolite layer may impose mass transfer resistance between the tightly packed crystals in continuous-flow catalysis. In this work, to ensure good mass transfer, a synthesis time of 3 h was preferred to produce amorphous silica gel which was served as the zeolite precursor for preparing ZSM-5 coating on SiC foams, improving the inter-crystal porosity of coatings.

After the modification of SiC foams with the precursor gel, thermal treatment was applied to cure the precursor dispersion to enhance the interaction between the support and precursor. Three curing temperatures of 30, 80 and $200 \text{ }^\circ\text{C}$ were studied in this work, showing that the temperature of the thermal treatment affected the morphology of the supported zeolite precursor (Fig. S4). Such changes suggest that phase change of the dispersed precursor, *i.e.* further crystallisation, occurred to some extent during curing, depending on the temperature used. The resulting ZSM-5 coatings on SiC foams (after the secondary growth

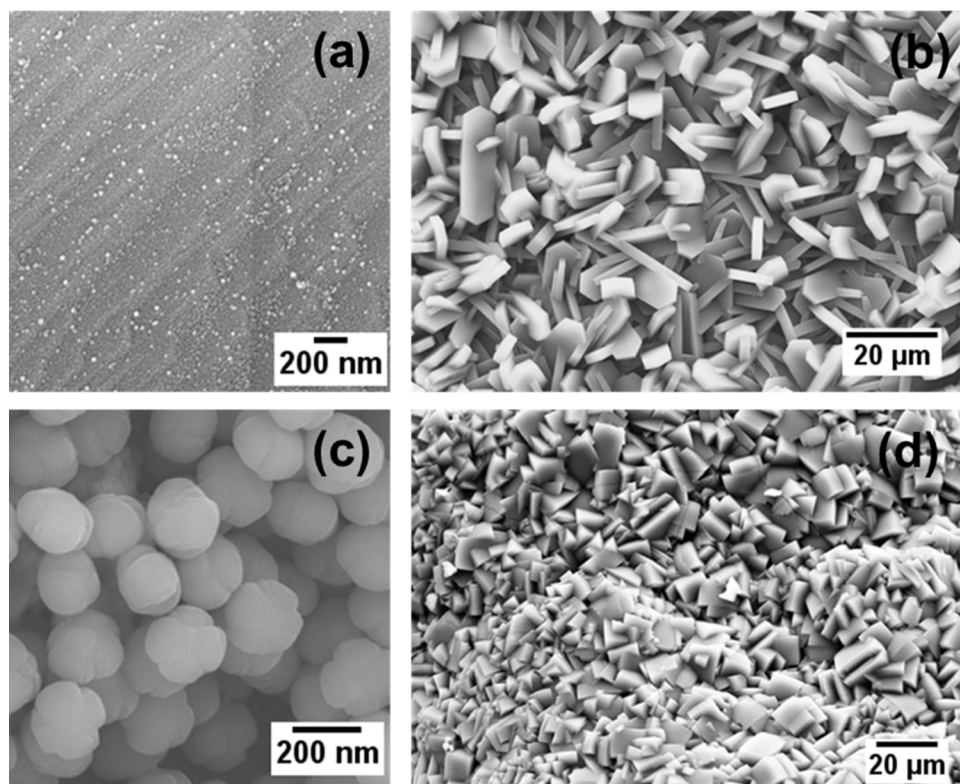


Fig. 2. Morphologies by SEM for (a) ZSM-5 precursors hydrothermally synthesised after 3 h and (b) the corresponding ZSM-5 coatings on SiC foams after the secondary growth synthesis; Morphologies by SEM for (c) ZSM-5 precursors hydrothermally synthesised after 8 h and (d) the corresponding ZSM-5 coatings on SiC foams after the secondary growth synthesis.

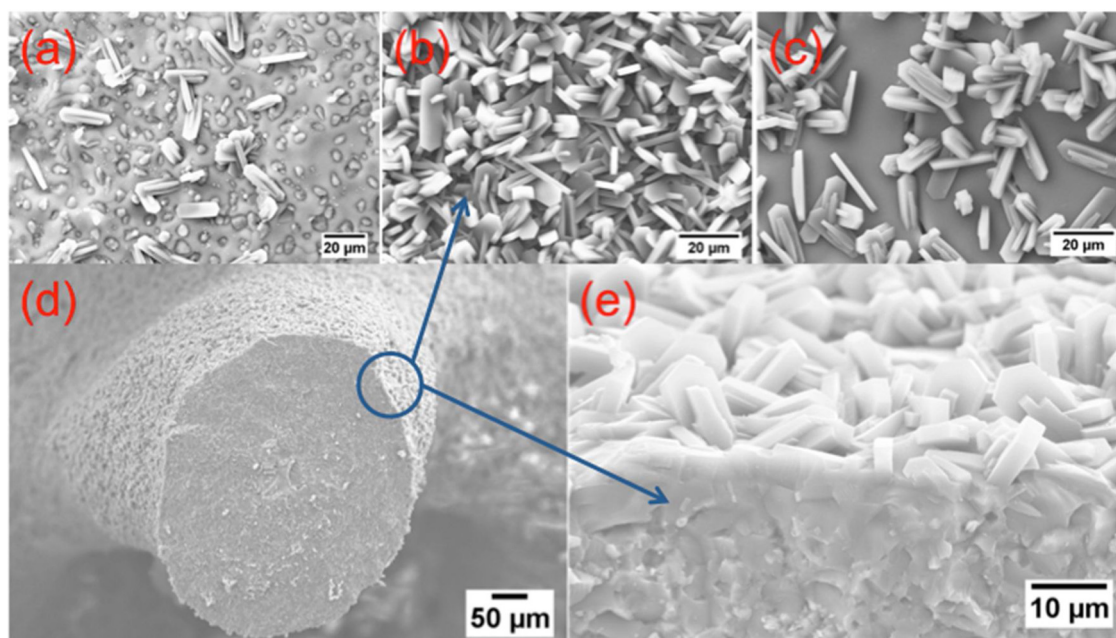


Fig. 3. SEM images of ZSM-5/SiC foam catalysts synthesised with zeolite precursors cured at (a) 30 °C; (b) 80 °C and (c) 200 °C; (d) a cross-section of the ZSM-5/SiC foam catalyst (precursor heat treatment at 80 °C) and (e) its ZSM-5 coating layer.

synthesis at 175 °C for 48 h) were characterised by SEM, as depicted in Fig. 3, showing different coating morphologies as well. It was found that the thermal treatment of the precursor at 80 °C was appropriate to enable the transformation of the dispersed zeolite precursor into a continuous layer of crystalline coating on the surface of SiC foams. Conversely, only discrete ZSM-5 crystals were formed by the zeolite precursors which were treated thermally at 30 °C and 200 °C.

The influence of the thermal treatment temperature (of the dispersed zeolite precursor on SiC foams) on the morphology of the

zeolitic coatings can be explained by the dissolution-recrystallisation mechanism [26,42]. The low temperature of 30 °C used for treating the precursor was too mild to further crystallise the zeolite precursor during the curing (Fig. S4a). Therefore, in the secondary growth synthesis, a fast dissolution of the precursor into the liquid phase occurred, facilitating the crystal growth in the liquid phase instead of on the surface of SiC foam (Figs. 3a and S5). When a high temperature of 200 °C was applied to the precursor, its full crystallisation was promoted during the thermal treatment (Fig. S4c), which might make the dissolution of the

crystallised precursor (into the secondary growth solution) difficult. In this case (with the thermally treated precursor at 200 °C), since there was a low concentration of silica near the surface, recrystallisation was unlikely to occur in the precursor layer. Therefore, discrete ZSM-5 crystals were formed due to the fully crystallised seeds (which were produced by treating the precursor thermally at 200 °C). Conversely, for the zeolite precursor thermally treated at 80 °C, an optimal rate of dissolution and recrystallisation could be achieved. At the initial stage of the secondary growth synthesis, the dispersed precursor on SiC foams dissolved under the alkaline condition at 175 °C, concentrating the local silica source, and hence promoting the uniform formation of nuclei on the SiC surface and, subsequently, a full coverage of ZSM-5 crystals on the SiC foam [53] (Fig. 3d). The ZSM-5 zeolite coating with highly crystalline phases (Fig. S6) via the compatible dissolution-recrystallisation route is different from that prepared by the seed-mediated secondary growth. The former promoted the formation of inter-crystal pores (which may be beneficial to the gas-to-solid mass transfer Fig. 3e), whereas the latter tended to produce the morphology of intergrown and dense coating (Fig. 2d). In conclusion, the ZSM-5/SiC foam sample, whose zeolite precursor was thermally pre-treated at 80 °C, was selected as the candidate structured catalyst for the catalytic study because the high-quality zeolite coating as formed on the surface of SiC foams, theoretically, facilitating the catalysis.

3.2. Comparative catalytic study of catalysts in upgrading bio-oil model compounds

A comparative study of methanol upgrading to hydrocarbons (at 400 °C) over the ZSM-5/SiC foam catalyst and the ZSM-5 pellets catalyst was performed with the results shown in Fig. 4. During the experiment, methanol was firstly dehydrated into dimethyl ether and water, followed by the production of hydrocarbons from the equilibrium mixture of the two oxygenates (*i.e.* methanol and dimethyl ether) [54]. Since dimethyl ether was always simultaneously present during the process and in near equilibrium with methanol [55], it is considered to be at an equivalent concentration to the unconverted methanol in this work. At WHSV of 8 h⁻¹, the ZSM-5/SiC foam catalyst shows the

comparatively high conversion of methanol from ~100% to ~55% over 270 min on stream. In addition to the high activity, it also shows high selectivity to light olefins (C₂–C₄), around 50–55% at WHSV of 8 h⁻¹ (Fig. 4c). Aromatic hydrocarbons were also produced in the methanol upgrading process, mainly were xylenes and styrene. Conversely, the ZSM-5 catalyst pellets show the relatively poor catalytic performance concerning the methanol conversion, *i.e.* 1.5–4.5% at 8 h⁻¹, though most of the products were light olefins as well (Fig. 4b and Fig. 4d). By considering the mass percent of the zeolite phase on the ZSM-5/SiC foam catalyst (*i.e.* about 9.5 wt.%), the textural properties of the supported ZSM-5 phase on SiC foams and the bulk ZSM-5 pellets are comparable (as shown in Table S2). Therefore, the enhanced catalytic performance achieved by the ZSM-5/SiC catalyst can be attributed to the improved global mass transfer rate in the foam bed, which has been proved by our previous work [56]. It is suggested that the advantages of using the ZSM-5/SiC foam catalyst include (i) the high open porosity of cellular foams as well as the stochastic cells in the foam matrix enhances global mass and momentum transfers due to the improved axial/radial mixing and low-pressure drop [32–34,56] and (ii) the zeolite coating with the inter-crystal porosity facilitates the local mass transfer in the catalyst layer. On the other hand, the restricted mass transfer across the ZSM-5 catalyst pellets suppresses the methanol conversion and causes the polymerisation of hydrocarbons (*i.e.* coking) [26,30].

Anisole is one of the typical oxygenated aromatic compounds derived from lignin. It exists in the aromatic compounds mixtures of bio-oils. In addition, anisole is much more refractory than the aliphatic oxygenates in bio-oils [46,57]. When the ZSM-5 catalyst pellets were used for anisole upgrading, at WHSV of 5 h⁻¹, the system showed insignificant activity to crack anisole, *i.e.* 2.9% conversion at 30 min on stream then thereafter the catalyst completely deactivated. When the ZSM-5/SiC foam catalyst was used instead, at WHSV of 5 h⁻¹, the initial conversion of anisole was significantly improved to 100%, as shown in Fig. 5. The ZSM-5/SiC foam catalyst lost its activity gradually during the operation and deactivated completely after 210 min on stream with the conversion dropped to zero. In the conversion of anisole via upgrading reactions, the major products were aromatic oxygenated compounds, such as methylanisole isomers and phenols.

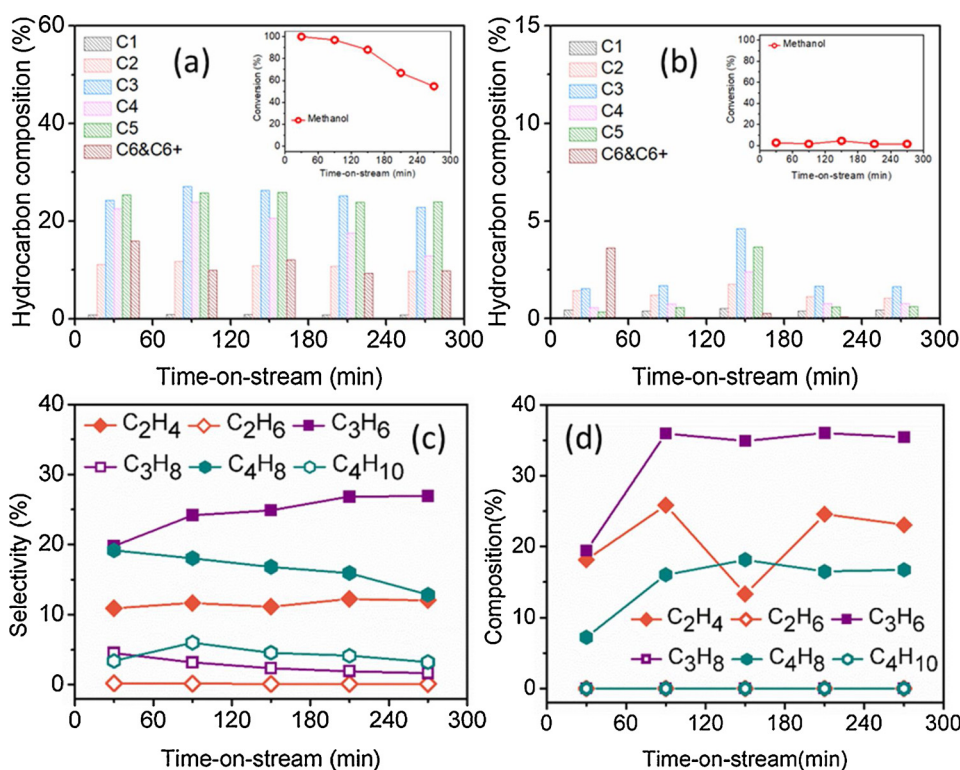


Fig. 4. Hydrocarbon compositions (C6&C6+: Paraffins, heavy olefins, naphthenes and aromatics containing six and more than six carbon atoms) and methanol conversion as a function of time-on-stream (ToS) at WHSV of 8 h⁻¹ over (a) the ZSM-5/SiC foam catalyst and (b) the ZSM-5 catalyst pellets; Selectivity to alkane and olefin as a function of ToS at WHSV of 8 h⁻¹ over (c) the ZSM-5/SiC foam catalyst and (d) the ZSM-5 pellets.

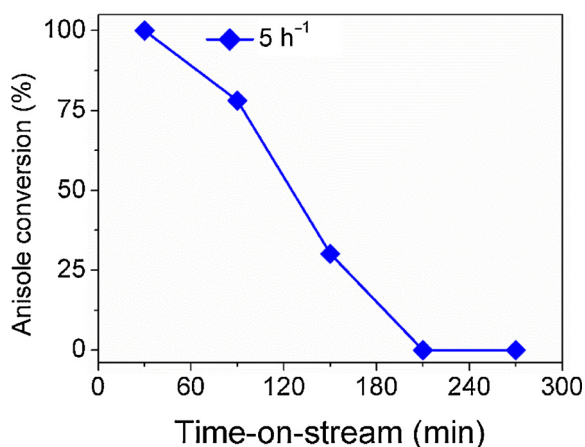


Fig. 5. Anisole conversion as a function of ToS at WHSV of 5 h^{-1} over the ZSM-5/SiC foam catalyst.

Table 1

Hydrocarbon compositions as a function of ToS at WHSV of 5 h^{-1} over the ZSM-5/SiC foam catalyst during anisole upgrading.^a

Products	Composition [%]		
	30 min	90 min	150 min
C1–C4 hydrocarbon	35.69	53.02	35.36
C5 hydrocarbon	2.89	5.29	0
Non-aromatic C6 hydrocarbon	5.70	7.52	5.09
Benzene	37.24	28.22	53.20
Toluene	8.41	4.17	6.35
Xylene	6.85	0	0
Styrene	3.22	3.27	0

^a The composition is with respect to the produced hydrocarbons and calculated by Eq. S2.

Hydrocarbons were the minor products and its distribution in the conversion of anisole over the ZSM-5/SiC foam catalyst were present in Table 1. The composition of all the products identified by in-line GC is present in Table S3. At 30 min, the main products identified by GC were benzene and C1–C4 hydrocarbons. Previous research [58] has found that anisole reacts easily through the cleavage of unimolecular $\text{CH}_3\text{-O}$ bonding, giving rise to the formation of methyl and phenoxy radicals together with the production of benzene and C1–C4 hydrocarbons. Polyphenolics might be produced at this stage [59], however, they were unable to be quantified due to the limited separation efficiency of the GC column used. At 90 min, the production of phenol increased significantly, whilst the yield of hydrocarbons decreased. Further increase of the yield of phenol and cresols was measured when reaction proceeded toward the catalyst deactivation. Possible explanations for the formation of C1–C4 hydrocarbons and methylbenzenes have been discussed in literature. Zhang et al. [60] proposed that hydrocarbons (*i.e.* alkanes and olefins) are potentially produced from methyl group polycondensation in anisole decomposition, and Pecullan [61] showed that hydrocarbons such as CH_4 , C_2H_4 and C_2H_6 are formed from radicals (*e.g.* methyl radical) produced pyrolytically. Additionally, hydrogen generation in anisole upgrading (*via* anisole pyrolysis [58,62], phenol pyrolysis [61] and/or the polycondensation reactions in anisole decomposition [60]) could also be the reason for the formation of C1–C4 hydrocarbons and methylbenzenes.

Previous work (upgrading of anisole over HY and HZSM-5 powders) [57,63] suggested that the deactivation of the catalysts during the conversion of anisole was mainly because of the condensation of anisole on the catalyst surface rather than the formation of polyaromatic coke. The intrinsic pore size of ZSM-5 (*ca.* 0.54 nm) limits the intracrystalline diffusion of anisole molecules. Therefore, anisole was prone to

condensate on the surface of ZSM-5 crystals during the reaction [59], which possibly applied to both ZSM-5/SiC foam and pelleted bulk ZSM-5 catalysts. Accordingly, the condensation of anisole would block the access to acid catalytic sites in the ZSM-5 crystalline phase resulting in the fast deactivation of the ZSM-5 catalysts. In comparison to the ZSM-5/SiC foam catalyst, the packed bed consisting of ZSM-5 pellets has a relatively poor global mass transfer, leading to a fast deactivation in this study. DSC analysis of the two deactivated catalysts from this work was carried out, and the results are shown in Fig. S7. Both catalysts showed an endotherm peak at $165 \text{ }^\circ\text{C}$ due to the pyrolysis of anisole, which is consistent with the previous findings [57,63], indicating the similar nature of the coke formed on the two catalysts in the catalytic anisole cracking.

The catalytic performance of the ZSM-5/SiC foam catalyst in the upgrading of methanol and anisole was affected adversely by the space velocity (WHSV). For methanol upgrading, when the WHSV was increased to 12 h^{-1} , the conversion dropped from an initial value of $\sim 94\%$ to $\sim 28\%$ after 270 min on stream (Fig. S8). However, in the case of anisole upgrading, the catalyst was immediately deactivated at WHSV of 10 h^{-1} . These findings are consistent with the report from Prasomsri et al. [57]. At a relatively high WHSV, *i.e.* a larger amount of anisole passing through the catalyst bed, more anisole molecules are likely to condense on the surface of the catalyst and hence causing a faster deactivation.

3.3. Deactivation of ZSM-5/SiC foam and ZSM-5 pellets catalysts

In zeolite catalysis, including bio-oils upgrading, the catalyst can be deactivated by active sites blocking and/or pore blocking [64]. The active sites blocking is due to the intrinsic nature of the zeolite catalyst, which can potentially be mitigated by engineering the local physical and chemical environments of the zeolitic framework [29]. The pore blocking is due to the formation of large amounts of carbonaceous species on the external surface of the catalyst, hindering the accessibility of active sites on the microspore surface. The pore blocking can be prevented to some extent by improving the global fluid-to-solid mass transfer steps. As anisole is a refractory model compound of bio-oils and severe deactivation was measured for the two catalysts under study, the deactivation of the ZSM-5/SiC foam catalyst and the ZSM-5 catalyst pellets in anisole upgrading was therefore further investigated. Additionally, it is worth noting that the water generated by the reactions may also cause the deactivation of the zeolite catalyst. Previous research showed that the water generated *in situ* caused the dealumination of ZSM-5 zeolites at the reaction temperature of about $400 \text{ }^\circ\text{C}$, and hence resulting in a decrease in the porosity and acidity of ZSM-5 zeolite [65]. Future research into this aspect is also needed.

The results of TGA of the spent catalysts from anisole upgrading are presented in Fig. 6. It shows that the weight loss of the two samples from 100 to $700 \text{ }^\circ\text{C}$ under air (after the activation of the catalysts at $100 \text{ }^\circ\text{C}$ for 2 h to remove the physisorbed water). The spent ZSM-5 pellets show the total weight-loss of *ca.* 5.0 wt.% at the end of TGA $< 600 \text{ }^\circ\text{C}$, whereas the weight loss of about 0.3 wt.% was measured for the spent ZSM-5/SiC foam catalyst, which is significantly less than the ZSM-5 pellets. The considerable difference in the total weight loss of the spent catalysts is consistent with the catalytic results, *i.e.* the relatively high activity and stability of ZSM-5/SiC foam catalyst in the anisole upgrading, indicating the global mass transfer in the ZSM-5/SiC foam catalyst was enhanced significantly, mitigating the coke formation.

The coke formation on the catalysts is expected to cause the deterioration of their textural structures, such as due to the pore blockage, which can prevent the access of reactants to active sites, lowering the catalytic activity [66]. Therefore, the effect of coke formation on the textural property of the spent catalysts was studied by N_2 physisorption in reference to the relevant fresh catalysts and the results are shown in Fig. 7 and Table 2. Both the fresh catalysts present the typical type I isotherm, confirming the microporous nature of the catalysts (for the

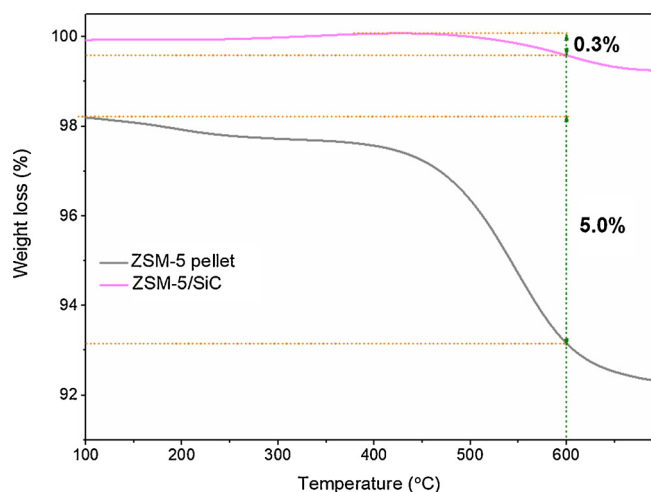


Fig. 6. TGA of the spent ZSM-5/SiC foam catalyst and ZSM-5 pellets catalyst from the catalytic anisole upgrading.

ZSM-5/SiC foam catalyst, it refers to the supported zeolite coating). After the reaction, the performance of N_2 physisorption of the two spent catalysts declined manifestly, especially for the spent ZSM-5 pellets, as evidenced by the reduced BET surface area of the spent catalysts in comparison to the fresh catalysts, *i.e.* from 34 to 17 $m^2 g^{-1}$ for the ZSM-5/SiC foam catalyst and from 386 to 85 $m^2 g^{-1}$ for the ZSM-5 pellets. The spent catalysts suffered a partial loss of micropores due to coke formation on the catalysts. The losses of micropore areas are calculated by the *t*-plot method for the spent catalysts as shown in Table 2. About 39% loss on the micropore area was measured for the spent ZSM-5/SiC foam while *ca.* 71% loss for the spent ZSM-5 pellets. The severe blockage of micropores in the spent ZSM-5 pellets is also confirmed by the analysis of the differential and cumulative micropore size distributions (as shown in Fig. S9).

The NH_3 -TPD analysis also reveals the effect of deactivation on the acidic property of the catalysts, as shown in Fig. 8 and Table 3. All catalysts exhibited two typical desorption peaks related to the weak (< 200 °C) and strong acidic sites (> 300 °C), respectively. In comparison to the concentration of the weak acidity, the presence of strong acidity in the fresh catalysts is relatively strong which agrees well with previous findings [67]. For cracking reactions, the weak acidic sites are believed to be of no catalytic importance, while the strong acidic sites are usually associated with the ammonia desorption from the Brønsted acid sites, being the main catalytic centres for deoxygenation reactions [60]. After deactivation, there are no significant changes measured for the concentration of weak acidity in the ZSM-5/SiC foam catalyst, while the number of strong acid sites dropped by about 60%. For the ZSM-5 pellets, the deactivation caused the decline of both strong (by 47%) and weak acidic sites (by 49%) in the spent catalyst.

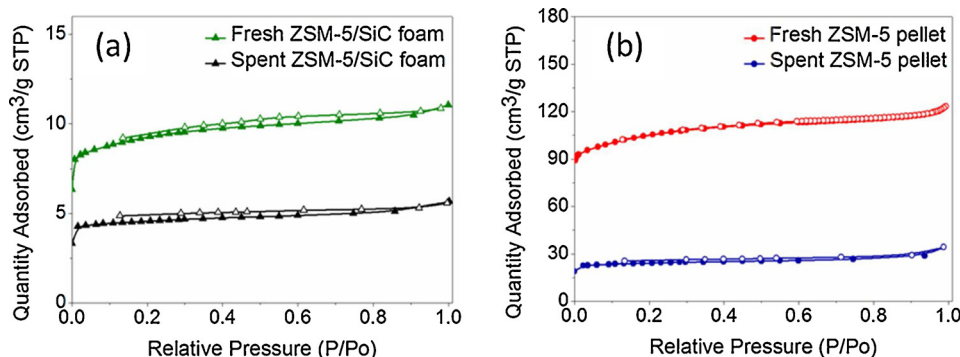


Fig. 7. N_2 adsorption-desorption isotherms of the fresh and spent (a) ZSM-5/SiC foam catalysts and (b) ZSM-5 catalyst pellets.

Müller et al. reported that the ZSM-5 zeolite deactivation at the initial stage of reactions (*i.e.* the methanol to olefins reactions) was the result of the blockage of Brønsted acid sites in the framework rather than the coke-induced pore blocking (which impedes the access of reactants to pores) [64]. Accordingly, the deactivation of the ZSM-5/SiC foam catalyst in the current system was likely due to the blockage of active sites, which is supported by the partial preservation of microporous structure, the comparably significant loss of strong acidity and the preservation of weak acidity (no catalytic importance). Conversely, for the ZSM-5 catalyst pellets, they might experience both deactivation mechanisms, especially the coke-induced pore blocking, according to the characterisation results discussed above. The poor mass transfer (*i.e.* the gas-to-solid and interparticle transfer) in packed beds using the catalyst pellets promoted fast carbon deposition on the surface of the pellets, resulting in the reduction of the accessibility to catalytic sites. Therefore, the comparatively better anti-deactivation performance of the zeolite/SiC foam catalysts is ascribed to the improved global mass transfer compared to the conventional pelletised zeolite catalysts. The spent ZSM-5/SiC foam catalyst can be regenerated by calcination (at 550 °C for 4 h). Anisole conversion by the regenerated ZSM-5/SiC foam catalyst was about 100% at WHSV of 5 h^{-1} over a reaction time of 30 min.

4. Conclusions

SiC foams have great importance in the field of heterogeneous catalysis and catalytic reaction engineering for process intensification. Based on the developed dispersion-based method, we presented the results of the ZSM-5 coating morphology on SiC foams by means of varying the zeolite precursor heat treatment (curing) temperature. The curing of the zeolite precursor on SiC foams at 80 °C was the most favourable process to obtain the high-quality ZSM-5 coating on SiC foams with the inter-crystal porosity. Proof-of-concept of using the structured ZSM-5/SiC foam catalyst for upgrading bio-oils was made. Comparative catalytic upgrading of bio-oil model compounds (*i.e.* methanol and anisole *via* deoxygenation reactions) over the ZSM-5/SiC foam catalyst and ZSM-5 pellets catalyst was performed. The structured ZSM-5/SiC foam catalyst showed comparatively superior catalytic performance than the ZSM-5 pellets regarding the conversions of methanol and anisole and the selectivity to light hydrocarbons. The catalyst deactivation was analysed by TGA, N_2 physisorption and NH_3 -TPD techniques, aimed at explaining the deactivation behaviours of the two catalysts. It was concluded that the enhanced mass/momentum transfers across the foam catalyst suppressed the deactivation due to carbon deposition on the external surface of the supported ZSM-5 coating appreciably. Conversely, the packed bed configuration using the ZSM-5 pellets suffered from both the blockage of active sites and micropores. Structured foam catalysts hold the promise for the future upgrade of industrial zeolite catalysis with still much room for improvement regarding the engineering of zeolite coating layers (*e.g.* the rational

Table 2
Specific surface areas of the fresh and spent ZSM-5/SiC foam catalyst and ZSM-5 pellets catalyst^a.

Sample	BET surface area [m ² g ⁻¹]	Micropore area ^b [m ² g ⁻¹]	Micropore area loss [%]	External surface area ^c [m ² g ⁻¹]	External surface area loss [%]
Fresh ZSM-5/SiC foam catalyst	34	23	–	11	–
Spent ZSM-5/SiC foam catalyst	17	14	39	3	73
Fresh ZSM-5 catalyst pellets	386	271	–	115	–
Spent ZSM-5 catalyst pellets	85	78	71	7	94

^a The information for ZSM-5/SiC foam catalyst is with respect to the total mass of the ZSM-5/SiC foam catalyst.

^b By the *t*-plot method.

^c By the subtraction of the micropore area from the BET surface area.

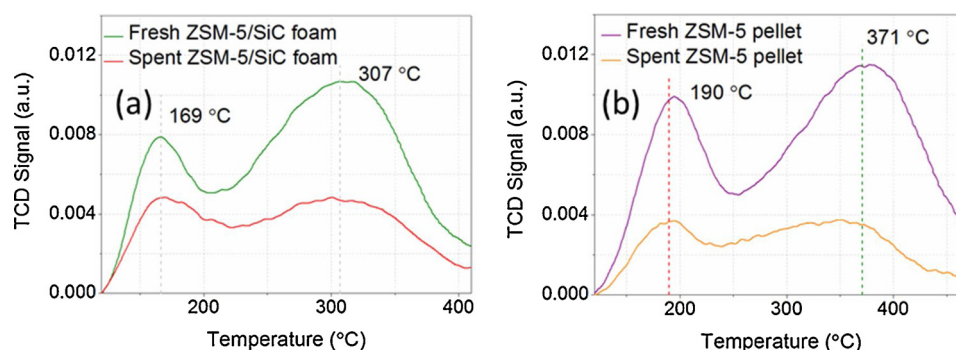


Fig. 8. NH₃-TPD spectra of the fresh and spent (a) ZSM-5/SiC foam catalysts and (b) ZSM-5 pellet catalysts (the absolute TCD signal is only related to the zeolite contents in the catalysts rather than the total mass of the catalysts, especially the ZSM-5/SiC foam catalyst).

Table 3
Analysis of NH₃-TPD data for ZSM-5/SiC foam catalyst and ZSM-5 pellets^a.

Catalyst	Peak temperature of desorption [°C]		Weak acidic sites [mmol g ⁻¹]	Strong acidic sites [mmol g ⁻¹]
	First peak	Second peak		
Fresh ZSM-5/SiC foam catalyst	169	307	0.005	0.020
Spent ZSM-5/SiC foam catalyst	169	307	0.005	0.008
Fresh ZSM-5 pellets	190	371	0.089	0.219
Spent ZSM-5 pellets	190	371	0.045	0.119

^a With respect to the total mass of the ZSM-5/SiC foam and ZSM-5 pellets catalysts.

design of porous and catalytic properties) and their interplay with the foam support geometry.

Credit author statement

The contribution of authors are:

XF, YJ, CW and CH conceptualised the research and provided resources for the work.

XO and KS performed the experimental work under the supervision of JZ, CH, YJ and XF.

XO drafted the initial manuscript.

CW, KS, JZ and XF helped the discussion.

CW, CH and XF revised the manuscript.

Declaration of Competing Interest

None.

Acknowledgements

This project has received funding from European Union's Horizon

2020 research and innovation programme under grant agreement No. 872102. The authors acknowledge the financial support from the Engineering and Physical Sciences Research Council for the research in structured foam catalysts (EP/R000670/1). X.F. and K.S. thank the financial support from The Royal Society for their research collaboration via the Royal Society International Exchanges award (IE161344). K.S. thanks the financial support for his research from the National Natural Science Foundation of China (51606106). Y.J. thanks the financial support from the Liaoning Provincial Natural Science Foundation of China (20180510012). YJ thanks the China Scholarship Council (CSC) for his academic visiting fellowship in the UK (file no. 201604910181).

Appendix A. Supplementary data

Supplementary material related to this article can be found, in the online version, at doi:<https://doi.org/10.1016/j.apcata.2020.117626>.

References

- [1] W.B. Widayatno, G. Guan, J. Rizkiana, J. Yang, X. Hao, A. Tsutsumi, A. Abudula, *Appl. Catal. B Environ.* 186 (2016) 166–172, <https://doi.org/10.1016/j.apcatb.2016.01.006>.
- [2] S. Vitolo, M. Seggiani, P. Frediani, G. Ambrosini, L. Politi, *Fuel* 78 (1999) 1147–1159, [https://doi.org/10.1016/S0016-2361\(99\)00045-9](https://doi.org/10.1016/S0016-2361(99)00045-9).
- [3] Q. Zhang, J. Chang, T. Wang, Y. Xu, *Energy Convers. Manage.* 48 (2007) 87–92, <https://doi.org/10.1016/j.enconman.2006.05.010>.
- [4] L. Zhang, R. Liu, R. Yin, Y. Mei, *Renew. Sust. Energy Rev.* 24 (2013) 66–72, <https://doi.org/10.1016/j.rser.2013.03.027>.
- [5] S. Xiu, A. Shahbazi, *Renew. Sust. Energy Rev.* 16 (2012) 4406–4414, <https://doi.org/10.1016/j.rser.2012.04.028>.
- [6] P.G. Levi, J.M. Cullen, *Environ. Sci. Technol.* 52 (2018) 1725–1734, <https://doi.org/10.1021/acs.est.7b04573>.
- [7] A.V. Bridgwater, *Biomass Bioenergy* 38 (2012) 68–94, <https://doi.org/10.1016/j.biombioe.2011.01.048>.
- [8] D.C. Elliott, G.G. Neuenschwander, T.R. Hart, J. Hu, A.E. Solana, C. Cao, A.V. Bridgwater, D.G.B. Boocock, *Science in Thermal and Chemical Biomass Conversion*, CPL Press, Thatcham, 2006, pp. 1536–1546.
- [9] A.V. Bridgwater, *Environ. Prog. Sustain. Energy* 31 (2012) 261–268, <https://doi.org/10.1002/ep.11635>.
- [10] S. Wang, Q. Cai, X. Wang, L. Zhang, Y. Wang, Z. Luo, *Energy Fuels* 28 (2014) 115–122, <https://doi.org/10.1021/ef4012615>.
- [11] H.J. Park, J.-K. Jeon, D.J. Suh, Y.-W. Suh, H.S. Heo, Y.-K. Park, *Catal. Surv. Asia* 15

- (2011) 161–180, <https://doi.org/10.1007/s10563-011-9119-7>.
- [12] Y. Uemura, N.T.T. Tran, S.R. Naqvi, N. Nishiyama, AIP Conf. Proc. 1877 (2017) 020002, <https://doi.org/10.1063/1.4999852>.
- [13] S. Vitolo, B. Bresci, M. Seggiani, M.G. Gallo, Fuel 80 (2001) 17–26, [https://doi.org/10.1016/S0016-2361\(00\)0063-6](https://doi.org/10.1016/S0016-2361(00)0063-6).
- [14] A. Veses, B. Puértolas, J.M. López, M.S. Callén, B. Solsona, T. García, ACS Sustainable Chem. Eng. 4 (2016) 1653–1660, <https://doi.org/10.1021/acscuschemeng.5b01606>.
- [15] A. Corma, G.W. Huber, L. Sauvanaud, P. O'Connor, J. Catal. 247 (2007) 307–327, <https://doi.org/10.1016/j.jcat.2007.01.023>.
- [16] F. Gong, Z. Yang, C. Hong, W. Huang, S. Ning, Z. Zhang, Y. Xu, Q. Li, Bioresour. Technol. 102 (2011) 9247–9254, <https://doi.org/10.1016/j.biortech.2011.07.009>.
- [17] F. Li, S. Ding, Z. Wang, Z. Li, L. Li, C. Gao, Z. Zhong, H. Lin, C. Chen, Energy Fuels 32 (2018) 5910–5922, <https://doi.org/10.1021/acs.energyfuels.7b04150>.
- [18] P.M. Mortensen, J.D. Grunwaldt, P.A. Jensen, K.G. Knudsen, A.D. Jensen, Appl. Catal. A Gen. 407 (2011) 1–19, <https://doi.org/10.1016/j.apcata.2011.08.046>.
- [19] H. Wan, R.V. Chaudhari, B. Subramaniam, Energy Fuels 27 (2013) 487–493, <https://doi.org/10.1021/ef301400c>.
- [20] A. Sassi, M.A. Wildman, H.J. Ahn, P. Prasad, J.B. Nicholas, J.F. Haw, J. Phys. Chem. B 106 (2002) 2294–2303, <https://doi.org/10.1021/jp013392k>.
- [21] P. Losch, A.B. Pinar, M.G. Willinger, K. Soukup, S. Chavan, B. Vincent, P. Pale, B. Louis, J. Catal. 345 (2011) 17–23, <https://doi.org/10.1016/j.jcat.2016.11.005>.
- [22] S. Ivanova, B. Louis, B. Madani, J.-P. Tessonnier, M. Ledoux, C. Pham-Huu, J. Phys. Chem. C 111 (2007) 4368–4374, <https://doi.org/10.1021/jp067535k>.
- [23] S. Mintova, V. Valchev, Zeolites 16 (1996) 31–34, [https://doi.org/10.1016/0144-2449\(95\)00078-X](https://doi.org/10.1016/0144-2449(95)00078-X).
- [24] R. Sharma, N. Bakhshi, Bioresour. Technol. 35 (1991) 57–66, [https://doi.org/10.1016/0960-8524\(91\)90082-U](https://doi.org/10.1016/0960-8524(91)90082-U).
- [25] Y. Fan, Y. Cai, X. Li, H. Yin, J. Xia, J. Ind. Eng. Chem. 46 (2017) 139–149, <https://doi.org/10.1016/j.jiec.2016.10.024>.
- [26] Y. Jiao, C. Jiang, Z. Yang, J. Zhang, Microporous Mesoporous Mater. 162 (2012) 152–158, <https://doi.org/10.1016/j.micromeso.2012.05.034>.
- [27] N.Y. Chen, T.Y. Yan, Ind. Eng. Chem. Process Des. Dev. 25 (1986) 151–155, <https://doi.org/10.1021/i200032a023>.
- [28] S. Ivanova, C. Lebrun, E. Vanhaecke, C. Pham-Huu, B. Louis, J. Catal. 265 (2009) 1–7, <https://doi.org/10.1016/j.jcat.2009.03.016>.
- [29] Y. Jiao, S. Xu, C. Jiang, M. Perdjón, X. Fan, J. Zhang, Appl. Catal. A Gen. 559 (2018) 1–9, <https://doi.org/10.1016/j.apcata.2018.04.006>.
- [30] Y. Jiao, X. Fan, M. Perdjón, Z. Yang, J. Zhang, Appl. Catal. A Gen. 545 (2017) 104–112, <https://doi.org/10.1016/j.apcata.2017.07.036>.
- [31] Y. Jiao, C. Jiang, Z. Yang, J. Liu, J. Zhang, Microporous Mesoporous Mater. 181 (2013) 201–207, <https://doi.org/10.1016/j.micromeso.2013.07.013>.
- [32] X. Fan, X. Ou, F. Xing, G.A. Turley, P. Denissenko, M.A. Williams, N. Batail, C. Pham, A.A. Lapkin, Catal. Today 278 (2016) 350–360, <https://doi.org/10.1016/j.cattod.2015.12.012>.
- [33] X. Ou, X. Zhang, T. Lowe, R. Blanc, M.N. Rad, Y. Wang, N. Batail, C. Pham, N. Shokri, A.A. Garforth, P.J. Withers, X. Fan, Mater. Charact. 123 (2017) 20–28, <https://doi.org/10.1016/j.matchar.2016.11.013>.
- [34] X. Ou, S. Xu, J.M. Warnett, S.M. Holmes, A. Zaheer, A.A. Garforth, M.A. Williams, Y. Jiao, X. Fan, Chem. Eng. J. 312 (2017) 1–9, <https://doi.org/10.1016/j.cej.2016.11.116>.
- [35] P. Losch, M. Boltz, K. Soukup, I.H. Song, H. Yun, B. Louis, Microporous Mesoporous Mater. 188 (2014) 99–107, <https://doi.org/10.1016/j.micromeso.2014.01.008>.
- [36] S. Ivanova, B. Louis, M.-J. Ledoux, C. Pham-Huu, J. Am. Chem. Soc. 129 (2007) 3383–3391, <https://doi.org/10.1021/ja0686209>.
- [37] J. Sterte, J. Hedlund, D. Creaser, O. Öhrman, W. Zheng, M. Lassinantti, Q. Li, F. Jareman, Catal. Today 69 (2001) 323–329, [https://doi.org/10.1016/S0920-5861\(01\)00385-6](https://doi.org/10.1016/S0920-5861(01)00385-6).
- [38] G.B.F. Seijger, O.L. Oudshoorn, W.E.J. van Kooten, J.C. Jansen, H. van Bekkum, C.M. van den Bleek, H.P.A. Calis, Microporous Mesoporous Mater. 39 (2000) 195–204, [https://doi.org/10.1016/S1387-1811\(00\)00196-7](https://doi.org/10.1016/S1387-1811(00)00196-7).
- [39] F.-C. Buciuman, B. Kraushaar-Czarnetzki, Catal. Today 69 (2001) 337–342, [https://doi.org/10.1016/S0920-5861\(01\)00387-X](https://doi.org/10.1016/S0920-5861(01)00387-X).
- [40] M. Kanezashi, J. O'Brien, Y. Lin, J. Membr. Sic. 286 (2006) 213–222, <https://doi.org/10.1016/j.memsci.2006.09.038>.
- [41] S. Lopez-Orozco, A. Inayat, A. Schwab, T. Selvam, W. Schwieger, Adv. Mater. 23 (2011) 2602–2615, <https://doi.org/10.1002/adma.201100462>.
- [42] Y. Jiao, X. Yang, C. Jiang, C. Tian, Z. Yang, J. Zhang, J. Catal. 332 (2015) 70–76, <https://doi.org/10.1016/j.jcat.2015.09.002>.
- [43] P.M. Budd, G.J. Myatt, C. Price, S.W. Carr, Zeolites 14 (1994) 198–202, [https://doi.org/10.1016/0144-2449\(94\)90155-4](https://doi.org/10.1016/0144-2449(94)90155-4).
- [44] G.J. Myatt, P.M. Budd, C. Price, S.W. Carr, J. Mater. Chem. 2 (1992) 1103–1104, <https://doi.org/10.1039/JM9920201103>.
- [45] M.-K. Jung, M.-H. Kim, S.-S. Hong, Microporous Mesoporous Mater. 26 (1998) 153–159, [https://doi.org/10.1016/S1387-1811\(98\)00227-3](https://doi.org/10.1016/S1387-1811(98)00227-3).
- [46] P.A. Horne, P.T. Williams, Renew. Energy 7 (1996) 131–144, [https://doi.org/10.1016/0960-1481\(96\)85423-1](https://doi.org/10.1016/0960-1481(96)85423-1).
- [47] T.M. Sankaranarayanan, A. Berenguer, C. Ochoa-Hernández, I. Moreno, P. Jana, J.M. Coronado, D.P. Serrano, P. Pizarro, Catal. Today 243 (2015) 163–172, <https://doi.org/10.1016/j.cattod.2014.09.004>.
- [48] H. Wang, M. Feng, B. Yang, Green Chem. 19 (2017) 1668–1673, <https://doi.org/10.1039/C6GC03198F>.
- [49] J. Mastelić, I. Jerković, Food Chem. 80 (2003) 135–140, [https://doi.org/10.1016/S0308-8146\(02\)00346-1](https://doi.org/10.1016/S0308-8146(02)00346-1).
- [50] Y. Yan, M.E. Davis, G.R. Gavalas, Ind. Eng. Chem. Res. 34 (1995) 1652–1661, <https://doi.org/10.1021/ie00044a018>.
- [51] S.M. Al-Jubouri, D.A. de Haro-Del Río, A. Alfutimie, N.A. Curry, S.M. Holmes, Microporous Mesoporous Mater. 268 (2018) 109–116, <https://doi.org/10.1016/j.micromeso.2018.04.023>.
- [52] E.A. Okoronkwo, P.E. Imoisili, S.A. Olubayode, S.O. Olusunle, Adv. Nanopart. 5 (2016) 135–139, <https://doi.org/10.4236/anp.2016.52015>.
- [53] B. Zheng, Y. Wan, W. Yang, F. Ling, H. Xie, X. Fang, H. Guo, Chin. J. Catal. 35 (2014) 1800–1810, [https://doi.org/10.1016/S1872-2067\(14\)60089-9](https://doi.org/10.1016/S1872-2067(14)60089-9).
- [54] M. Bjørgen, S. Svelle, F. Joensen, J. Nerlov, S. Kolboe, F. Bonino, L. Palumbo, S. Bordiga, U. Olsbye, J. Catal. 249 (2007) 195–207, <https://doi.org/10.1016/j.jcat.2007.04.006>.
- [55] M. Bjørgen, F. Joensen, M.S. Holm, U. Olsbye, K.-P. Lillerud, S. Svelle, Appl. Catal. A Gen. 345 (2008) 43–50, <https://doi.org/10.1016/j.apcata.2008.04.020>.
- [56] Y. Jiao, X. Ou, J. Zhang, X. Fan, React. Chem. Eng. 4 (2019) 427–435, <https://doi.org/10.1039/C8RE00215K>.
- [57] T. Prasomsri, A.T. To, S. Crossley, W.E. Alvarez, D.E. Resasco, Appl. Catal. B Environ 106 (2011) 204–211, <https://doi.org/10.1016/j.apcatb.2011.05.026>.
- [58] M. Nowakowska, O. Herbinet, A. Dufour, P.-A. Glaude, Combust. Flame 161 (2014) 1474–1488, <https://doi.org/10.1016/j.combustflame.2013.11.024>.
- [59] I.S. Graça, R.-D. Comparot, S.B. Laforge, P. Magnoux, J.M. Lopes, M.F. Ribeiro, F. Ramôa Ribeiro, Energ. Fuel. 23 (2009) 4224–4230, <https://doi.org/10.1021/ef9003472>.
- [60] J. Zhang, B. Fidalgo, A. Kolios, D. Shen, S. Gu, Chem. Eng. J. 336 (2018) 211–222, <https://doi.org/10.1016/j.cej.2017.11.128>.
- [61] M.S. Pecullan, Pyrolysis and Oxidation Kinetics of Anisole and Phenol, Doctoral Dissertation, Princeton University, 1997.
- [62] R.H. Schlosberg, P.F. Szajowski, G.D. Dupre, J.A. Danik, A. Kurs, T.R. Ashe, W.I. Olmstead, Fuel 62 (1983) 690–694, [https://doi.org/10.1016/0016-2361\(83\)90308-3](https://doi.org/10.1016/0016-2361(83)90308-3).
- [63] S. Du, D.P. Gamliel, M.V. Giotto, J.A. Valla, G.M. Bolas, Appl. Catal. A Gen. 513 (2016) 67–81, <https://doi.org/10.1016/j.apcata.2015.12.022>.
- [64] S. Müller, Y. Liu, M. Vishnuvarthan, X. Sun, A.C. van Veen, G.L. Haller, M. Sanchez-Sanchez, J.A. Lercher, J. Catal. 325 (2015) 48–59, <https://doi.org/10.1016/j.jcat.2015.02.013>.
- [65] A.G. Gayubo, A.T. Aguayo, M. Olazar, R. Vivanco, J. Bilbao, Chem. Eng. Sci. 58 (23–24) (2003) 5239–5249, <https://doi.org/10.1016/j.ces.2003.08.020>.
- [66] P. Dejaifve, A. Auroux, P.C. Gravelle, J.C. Védrine, Z. Gabelica, E. Derouane, J. Catal. 70 (1981) 123–136, [https://doi.org/10.1016/0021-9517\(81\)90322-5](https://doi.org/10.1016/0021-9517(81)90322-5).
- [67] L. Rodríguez-González, F. Hermes, M. Bertmer, E. Rodríguez-Castellón, A. Jiménez-López, U. Simon, Appl. Catal. A Gen. 328 (2007) 174–182, <https://doi.org/10.1016/j.apcata.2007.06.003>.